



Electrochemical and Biological Studies of Synthesized Schiff base and It's Zinc Complex

REKHA SHARMA, VINAYAK GUPTA, SMRITI SINGH,
ISHWAR CHAND BALAEE and SARITA VARSHNEY*

Department of Chemistry, University of Rajasthan, Jaipur-302004, India.

*Corresponding author E-mail: rsharmagck@gmail.com

<http://dx.doi.org/10.13005/ojc/380603>

(Received: May 17, 2022; Accepted: December 12, 2022)

ABSTRACT

The present paper investigated the electrochemical behaviour of Schiff base and its zinc complex at a working electrode by cyclic voltammetry technique. In the phosphate and Britton-Robinson buffers, the electrochemical study of Schiff base was performed within various pH values 5-9. Cyclic voltammograms of the examined Schiff base exhibited irreversible and diffusion controlled waves at different sweep rates, which is associated with the two electron reduction process of azomethine group. The symmetry transfer coefficient (α_n), the diffusion coefficient ($D_0^{1/2}$) and rate constant ($k_{t,h}^0$) of the reactant species were calculated. Cyclic voltammetric study of zinc complex showed one electron diffusion controlled, quasi-reversible peaks at 50-250 mV/s sweep rates. Antimicrobial study of zinc complex showed that zinc complex found to be more potent than uncoordinated Schiff base.

Keywords: Amino acid, Schiff base, Cyclic voltammetry, Antimicrobial study.

INTRODUCTION

Schiff base ligands are azomethine containing functional groups which are easily synthesized through the condensation reaction of carbonyl compounds with primary amines and they are commonly prepared with heat or under acidic and basic catalysis¹⁻². Schiff base complexes have shown remarkable attention to various fields like catalysis³, sensors⁴, luminescent and non linear optical materials⁵. During the last decade, metal complexes and Schiff base ligand show a vast variety of biological activities including anticancer, antioxidant, antimicrobial, antibacterial and antifungal

properties⁶⁻¹⁰. Electrochemical evaluation have benefits due to their simplicity, more sensitivity, reduction in solvent, sample consumption, faster speed evaluation and minimum operating cost¹¹.

Sample preparation and Instrumentation

Amino acid-Schiff base (GMBPI) solutions with a concentration of 1mM Amino acid-Schiff base (GMBPI) solutions with a concentration of 1mM were prepared in methanol/DMF solvent. Buffer solutions have been prepared in deionized water. Zinc complex solution was prepared by mixing of 1mM of complex in DMF. For cyclic voltammetry study, the experimental solutions of GMBPI were

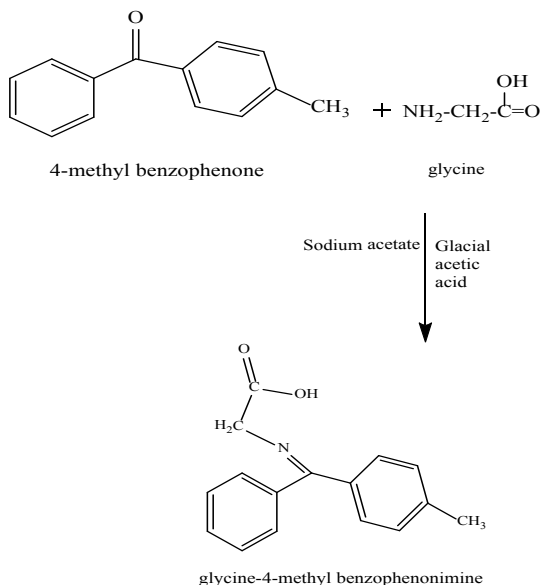


prepared by mixing of stock solution of GMBPI, methanol/DMF solvent and phosphate buffer/BR buffer of varying pH. The test solutions of complex consisted of stock solution of complex, DMF solvent and NaClO_4 as a supporting electrolyte in the cyclic voltammetric experiment.

Electrochemical measurements of GMBPI and its zinc complex have been carried out using 3-electrode cell containing glassy carbon (GCE) as working electrode, Pt as counter electrode and Ag/AgCl as reference electrode. By using alumina suspension, GCE was polished previous to every experiment¹². The experimental solutions of Schiff base ligand and complex were degassed by passing nitrogen gas for 15 min to remove the dissolved oxygen and were blanketed with the nitrogen gas during the experiments.

EXPERIMENTAL

Synthesis of amino acid-Schiff base-Glycine-4-methylbenzophenonimine (GMBPI) Schiff base was synthesized by mixing of sodium acetate and glycine amino acid in the glacial acetic acid solution of 4-methyl benzophenone¹³. The reaction solution was left under reflux. The reaction mixture was cooled and extracted. The product was separated by separating funnel and washed with plenty of hot ethanol and dried at room temperature.



Scheme 1. Structure of Synthesized glycine-4-methylbenzophenonimine (GMBPI)

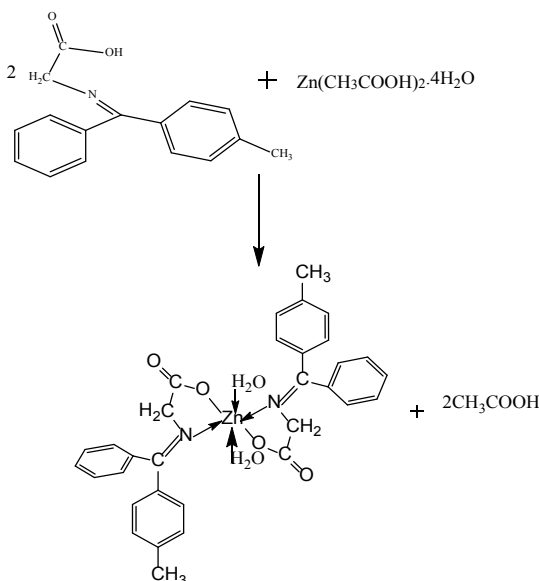
Synthesis of metal complex

The zinc complex of GMBPI was prepared by dropwise addition of the hot methanolic solution of glycine-4-methylbenzophenon-imine (GMBPI) to the methanolic solution of zinc acetate with constant stirring¹⁴. By refluxing the resulting mixture, the complex was formed. The obtained product was filtered, washed several times with ethanol and dried over CaCl_2 .

$$|E_p - E_{p/2}| = \frac{1.857RT}{\alpha_n F} = \left(\frac{47.7}{\alpha_n} \right) mV \quad (1)$$

$$I_p = 3.01 \times 10^5 n(\alpha_n)^{1/2} \text{ACD}_0^{1/2} \nu^{1/2} \quad (2)$$

$$E_p = -\frac{RT}{\alpha_n F} \left[0.78 + \ln \left(\frac{D_0^{1/2}}{k'_{f,s}} \right) + \ln \left(\frac{\alpha_n F \nu}{RT} \right)^{1/2} \right] \quad (3)$$



Scheme 2. Synthesis of Zn (II) complex of glycine-4-methylbenzophenonimine

RESULT AND DISCUSSION

Elemental analysis

Analytical records of amino acid-ketimine (GMBPI) and its zinc complex were carried out by micro analytical technique. Elemental analysis were found (cal.) for ligand (GMBPI): M. Wt.; 253.10 (253.30), C; 75.65 (75.87), H; 5.96 (5.97), N; 5.48 (5.53), O; 12.56 (12.63) and complex : M. Wt.; 632.05 (634.18), C; 64.32 (64.41), H; 5.70 (5.72), N; 4.34 (4.42), O; 14.96 (15.14), Zn; 10.12 (10.31).

Cyclic voltammetric study of amino acid-ketimine (GMBPI)

In the cyclic voltammetric study, the potential is applied at the GCE electrode and current is

measured. The symmetry-transfer coefficient (α_n) of the electrode reaction, rate constant (K_{fh}^o) and diffusion coefficient ($D_0^{1/2}$) were determined for irreversible electrode process of ketimine (GMBPI) with using following equations and data reported in Tables 1-3.

Cyclic voltammograms of GMBPI have been recorded on working electrode within the

range +1000mV to -1800 mV at varying sweep rates in methanol and DMF media containing phosphate and BR buffers (Fig. 1-9). All the voltammograms of amino acid-ketimine showed only well defined cathodic peaks in forward sweep rates, giving clue of two electrons in forward sweep rates, giving clue of two electron reduction process of azomethaine moiety.

Table 1: In methanol-phosphate buffer, the impact of sweep rates versus electrochemical parameters of 1mM amino acid-ketimine (GMBPI) at varying pH 5.8-8

pH	v(mV/s)	$E_{p,c}$ (mV)	$I_{p,c}$ (μ A)	$E_{p/2}$ (mV)	$I_{p,c}/v^{1/2}$	α_n	$D_0^{1/2}$ (cm ² /s)	k_{fh}^o (cm/s)
5.8	50	-829.46	11.98	-724.97	1.694228	0.456503	15.78437	1.28x10-8
	100	-844.57	18.82	-704.56	1.882	0.34069	20.29631	6.94x10-7
	150	-871.66	26.74	-710.52	2.183312	0.296016	25.26012	3.13x10-6
	200	-880.38	30.83	-712.12	2.18001	0.28349	25.77312	5.02x10-6
	250	-897.38	34.87	-705.19	2.205372	0.248192	27.8654	1.62x10-5
7	50	-834.03	13.81	-718.86	1.953029	0.41417	19.10277	5.38x10-8
	100	-856.71	22.57	-704.46	2.257	0.3133	25.38214	1.77x10-6
	150	-876.04	29.16	-709.13	2.380904	0.285783	28.03503	4.61x10-6
	200	-890.08	35.46	-707.32	2.507401	0.260998	30.89458	1.13x10-5
	250	-912.12	38.81	-708.59	2.45456	0.234363	31.91581	2.55x10-5
8	50	-845.43	15.67	-730.42	2.216073	0.41474	21.66056	4.99x10-8
	100	-875.97	26.02	-714.24	2.602	0.294936	30.15925	3.01x10-6
	150	-898.33	31.33	-712.46	2.558084	0.256631	31.78611	1.07x10-5
	200	-911.22	38.52	-631.88	2.723775	0.17076	41.49118	2.44x10-4
	250	-926.3	44.49	-704.34	2.813795	0.214904	38.20742	5.18x10-5

Table 2: In DMF-phosphate buffer, the impact of sweep rates versus electrochemical parameters of 1mM amino acid-ketimine (GMBPI) at varying pH 5.8-8

pH	v(mV/s)	$E_{p,c}$ (mV)	$I_{p,c}$ (μ A)	$E_{p/2}$ (mV)	$I_{p,c}/v^{1/2}$	α_n	$D_0^{1/2}$ (cm ² /s)	k_{fh}^o (cm/s)
5.8	50	-877.78	25.67	-776.11	3.630286	0.469165	33.36224	7.54x10-9
	100	-881.81	33.4	-781.13	3.34	0.473778	30.54471	7.78x10-9
	150	-885.53	43.21	-778.31	3.528082	0.44488	33.29619	2.54x10-8
	200	-897.92	52.71	-791.99	3.72716	0.450297	34.96274	2.07x10-8
	250	-907.58	56.32	-787.55	3.56199	0.397401	35.56768	1.21x10-7
7	50	-910.74	30.05	-820.77	4.249712	0.530177	36.73891	5.55x10-10
	100	-913.27	39.62	-828.72	3.962	0.564163	33.20391	2.07x10-10
	150	-930.86	45.25	-835.91	3.694647	0.50237	32.81243	1.51x10-9
	200	-989.3	54.35	-847.12	3.843125	0.33549	41.76589	3.59x10-7
	250	-1007.12	65.09	-857.47	4.116653	0.318744	45.89872	6.56x10-7
8	50	-940.81	28.81	-839.18	4.074349	0.46935	37.43581	2.66x10-9
	100	-961.19	36.21	-834.33	3.621	0.376005	37.17139	7.57x10-8
	150	-970.55	51.12	-839.58	4.173931	0.364206	43.53606	1.46x10-7
	200	-1008.36	61.11	-828.48	4.32113	0.265177	52.82101	4.97x10-6
	250	-1040.05	69.21	-754.45	4.377225	0.167017	67.42111	2.16x10-4

Table 3. In DMF-BR buffer, the impact of sweep rates versus electrochemical parameters of 1mM amino acid-ketimine (GMBPI) with using varying pH (5, 7 & 9)

pH	v(mV/s)	$E_{p,c}$ (mV)	$I_{p,c}$ (μ A)	$E_{p/2}$ (mV)	$I_{p,c}/v^{1/2}$	α_n	$D_0^{1/2}$ (cm ² /s)	k_{fh}^o (cm/s)
5	50	-1044.9	6.3	-970.56	2.071823	0.641646	7.001399	7.81x10-14
	100	-1063.35	9.08	-965.49	1.948	0.487431	8.186654	4.22x10-11
	150	-1090.21	13.07	-973.09	1.798742	0.407275	10.526	1.10x10-9
	200	-1121.5	16.71	-963.93	1.938887	0.302723	13.51812	8.20x10-8
7	50	-1050.68	6.9	-963.14	0.975807	0.544894	8.321188	3.88x10-12
	100	-1067.5	9.77	-967.1	0.977	0.4751	8.922353	7.00x10-11
	150	-1097.71	15.71	-941.76	1.282716	0.305867	14.59961	8.92x10-8
	200	-1126.94	20.14	-1003.71	1.424113	0.387081	14.40856	2.29x10-9
9	50	-1064	4.31	-990.86	0.609526	0.652174	4.751029	2.14x10-14
	100	-1087.63	8.03	-972.66	0.803	0.414891	7.8474	5.08x10-10
	150	-1134.95	10.53	-986.82	0.859771	0.322014	9.537229	1.88x10-8
	200	-1140.82	14.38	-952.07	1.01682	0.252715	12.73226	5.18x10-7

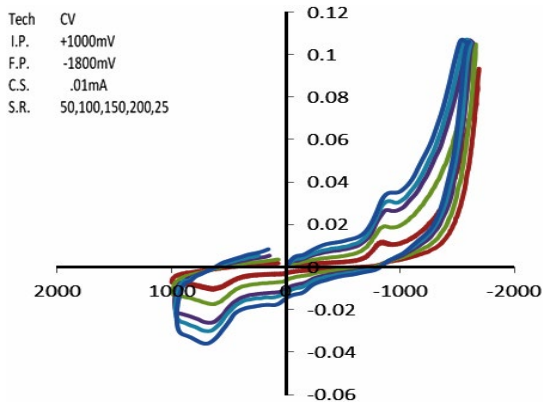


Fig. (1)

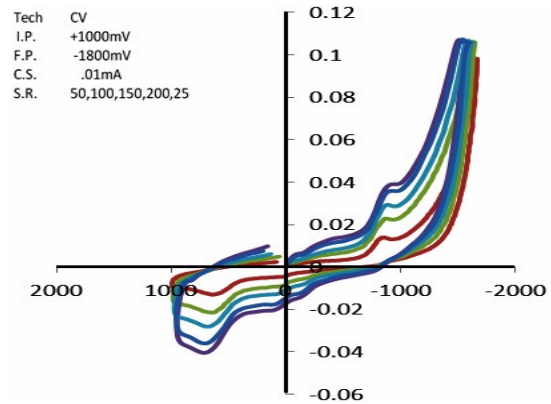


Fig. (2)

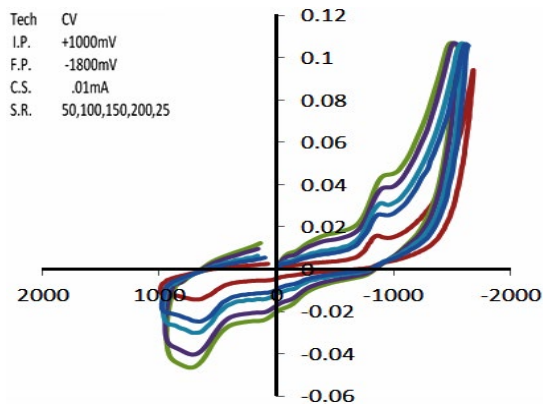


Fig. (3)

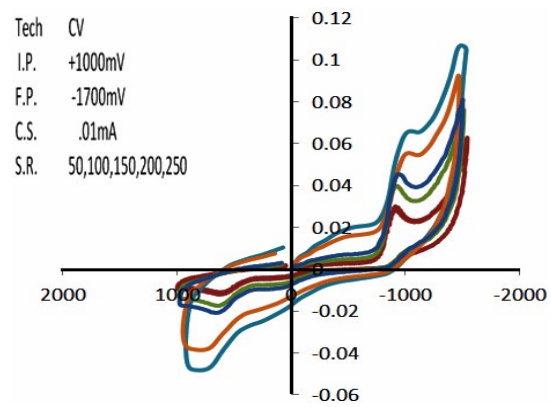


Fig. (4)

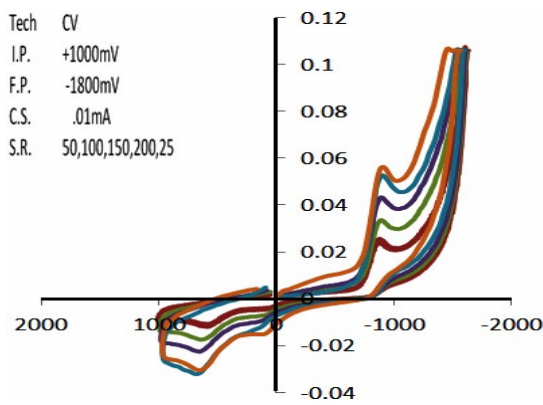


Fig. (5)

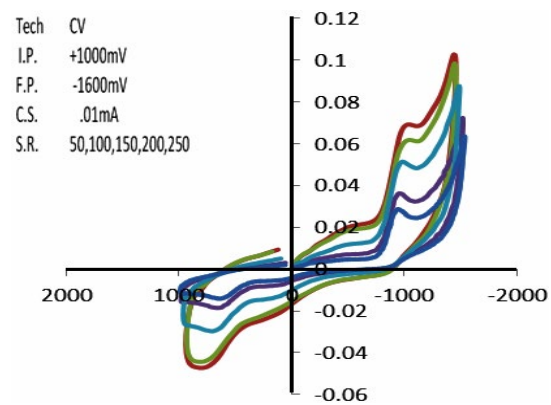


Fig. (6)

(A) In methanol-phosphate buffer, Fig. (1), (2) & (3) represent cyclic voltammograms of GMBPI with using different sweep rates at varying pH 5.8, 7 & 8 respectively.

(B) In DMF-phosphate buffer, Fig. (4), (5) & (6) represent cyclic voltammograms of GMBPI with using different sweep rates at varying pH

5.8, 7 & 8 respectively .

(C) In DMF-BR buffer, Fig. 7, 8 & 9 represent cathodic peak potential ($E_{p,c}$) versus cyclic voltammograms of GMBPI with using various sweep different sweep rates at varying rates at varying pH 8 pH 5, 7 & 9 respectively

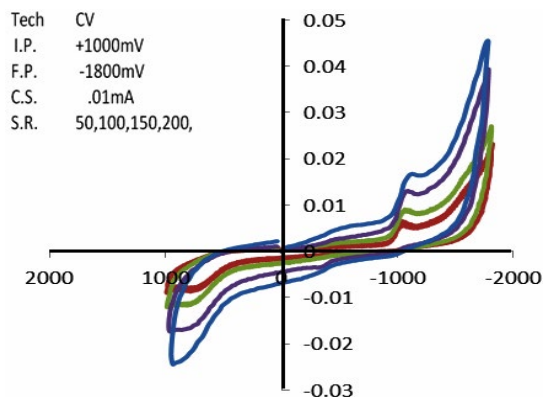


Fig. (7)

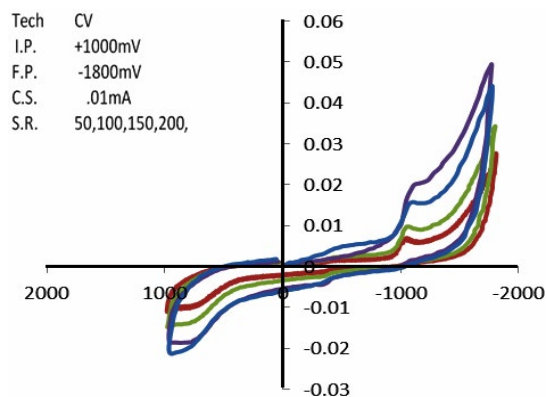


Fig. (8)

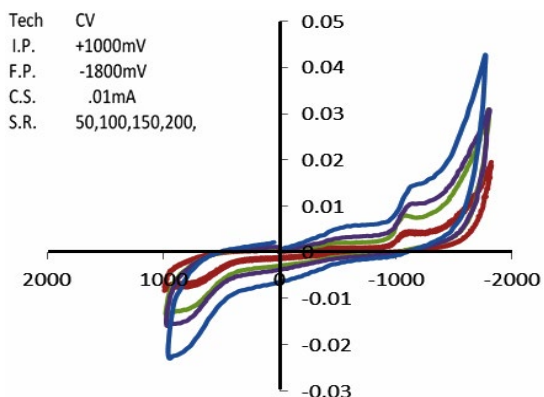


Fig. (9)

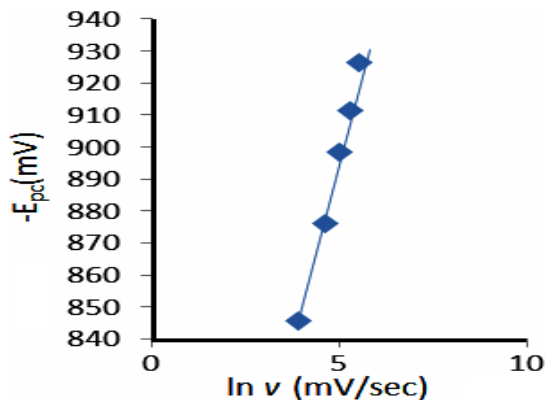


Fig. 10. In methanol-phosphate buffer cathodic peak potential ($E_{p,c}$) versus $\ln v$ of GMBPI with using various rates at pH 8

Now the effects of sweep rate, buffer, solvent and pH on reduction behavior of glycine-4-methyl benzophenimine have been discussed.

Impact of sweep rate

To observe the effect of sweep rate on reduction of ligand, it could be shown by recorded the cyclic voltammograms (Fig. 1-9) of amino acid-ketimine. At pH 5.8, the ligand showed cathodic reduction peaks with 50-250(mV/s) sweep rates from -829.46 mV to -897.38 mV in methanol-phosphate buffer. So, the reduction signal shifted towards high negative potential values with faster scan rate¹⁵. In Fig. 10, the cathodic peak potential and sweep rate response for ketimine depicted as $E_{p,c}$ versus $\ln v$ is linear, giving evidence for irreversible reduction process of GMBPI.

Impact of buffer

The electrochemical data of ligand strongly influenced from buffer solutions due to different polarity of buffer. Cyclic voltammograms were recorded for ligand in phosphate and BR buffers

with DMF solvent within pH range (5-9). The values of peak potential with a sweep rate of 100mV/s and pH 7 were measured -913.27 mV and -1067.5 mV respectively, in DMF-phosphate buffer and DMF-BR buffer. This indicates that the charge transfer process is easier in phosphate buffer comparison of BR buffer. In DMF-phosphate buffer, the cathodic peak potential values at pH 7 were increased from -910.74 mV to -1007.12 mV with using various sweep rates from 50 -250 mV/s and the deviation in cathodic peak current values were observed from 30.05 μ A to 65.09 μ A, indicating irreversibility of electrode process.

Impact of pH

The voltammetric behavior of GMBPI was investigated at different pH using cyclic voltammetric technique and data summarized in Tables 1, 2 & 3. The data indicated that as pH changed from 5-9 range, then reduction potential also changed. When pH modified from acidic to neutral, then the peak potential values of ligand have been displaced in

negative direction. In DMF-phosphate buffer, the values of reduction peak potential of ketimine with varying pH 5.8 and 7 (sweep rates 50-250mV/s) are -877.78, -881.81, -885.53, -897.92, -907.58 (mV) and -910.74, -913.27, -930.86, -989.3, -1007.12 (mV), respectively. These electrochemical records indicated more negative peak potential at higher pH, suggesting the involvement of proton during the reduction.

Impact of solvent

For observing the impact of solvent on voltammetric variables, comparative studies were done. For this purpose, in CH₃OH and DMF media using phosphate buffer, cyclic voltammograms of 1mM solution of ligand have been recorded. By using different pH (5.8, 7 & 8), the cathodic peak potential values in methanol vary from -829.46 mV to -926.3 mV with different sweep rates (50-250 mV/s). While in DMF, the reduction peak potential values measured from -877.78mV to -1040.05 mV, which related to the various sweep rates (50-250 mV/s). It showed that the electron transfer process was more easily in methanol than that of in DMF which could be accounted due to low viscosity of methanol than DMF¹⁶.

Electrochemical behavior of Zn (II) complex of GMBPI

For Zn complex (1mM), cyclic voltammograms were shown within the potential range +500 mV to -900 mV in Fig. 11 by using various sweep rates 50-250mV/s in DMF media using NaClO₄ as supporting electrolyte. From cyclic voltammograms, there was both cathodic peak and anodic peak occurring in forward and backward direction at all sweep rates. The separation peak potentials (ΔE_p) is greater than the theoretical Nernstian values (59mV) for an electrochemically reversible process and this is correspondence with the quasi-reversibility of Zn(II) complex.

For one electron transfer reduction process of Zn(II) to Zn(I) exposed to reduction sweep at -311.79, -326.34, -349.03, -356.34, -365.96 (mV) in forward direction with a corresponding oxidation sweep at -242.67, -230.78, -220.96, -204.92, -187.49 (mV) with sweep rates of 50, 100, 150, 200, 250 (mV/s) and described in Table 4. The separation potentials between reduction and oxidation peaks were 69.12, 95.56, 128.07, 151.42, 178.47 (mV). The peak current ratio ($I_{p,a}/I_{p,c}$) for zinc complex of GMBPI was 0.63, 0.625, 0.633, 0.695, 0.810 with various sweep rates from 50 to 250 (mV/s),

which were less than unity. These data indicated that redox behavior of the Zn(II) complex exhibited quasi-reversibility at all sweep rates¹⁷.

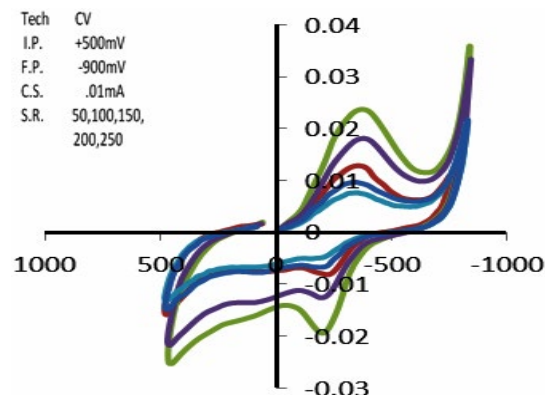


Fig. 11. In DMF-NaClO₄, cyclic voltammogram of Zinc complex of GMBPI with various sweep rates

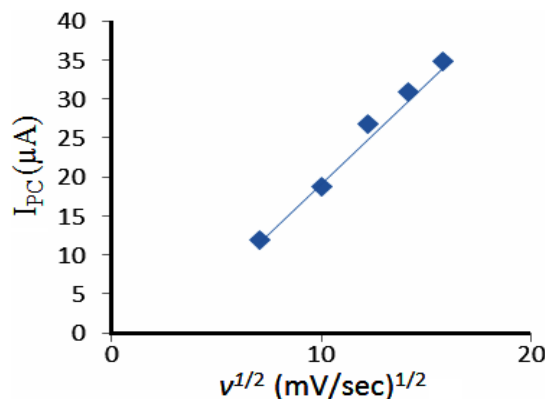


Fig. 12. Peak Current (I_{pc}) v/s $v^{1/2}$ of GMBPI in methanol-phosphate buffer pH (5.8)

The reduction peak current (I_{pc}) values increase with increasing value of the square root of the sweep rates. The graph is plotted between peak current values and the square root of sweep rate for GMBPI (Fig. 12) and linear graph is obtained. This illustrates that the reduction of GMBPI is a diffusion controlled process¹⁸. Infrared study-IR spectral of amino acid-ketimine ligand and its zinc complex were obtained in the region 4000-400 cm^{-1} . The vibration stretching band for the azomethine group was observed at 1620-1630 cm^{-1} in the spectral of Schiff base ligand. The stretching vibration bands for carbonyl group of 4-methylbenzophenone and -NH₂ group of amino acid were disappeared in the spectra of free ligand, indicating the condensation between ketonic and amino group take place. When zinc metal was complexed with GMBPI then this decreased

the frequency of C=N group, which attributed at 1590-1610 cm^{-1} , suggesting coordination of metal ion via the imine nitrogen¹⁹. In complexes, the bands appearing at 520-550 cm^{-1} and 430-470 cm^{-1} , which have been assigned to $\nu_{\text{M-O}}$ and $\nu_{\text{M-N}}$, respectively.

Antimicrobial study of ketimine and its Zinc complex

The synthesized ketimine (GMBPI) and its zinc complex were evaluated for antimicrobial activity. Amino acid-ketimine ligand and its zinc complex were explored for their biological screening against two bacterial species (*Bacillus subtilis*, *Escherichia coli*) and two fungal strains (*Penicillium chrysogenum*, *Aspergillus niger*) through disc diffusion method. All the samples were prepared in dimethyl sulfoxide (DMSO). The obtained results for antimicrobial activity were presented in Tables 5 & 6 and the data showed that the metal complex was found to be more active than free ligand. Increased activity of the complex is attributed due to chelation²⁰.

CONCLUSION

In the present paper, zinc complex of amino acid-ketimine ligand derived from amino acid and 4-methylbenzophenone was prepared. The electrochemical study of synthesized amino acid-ketimine showed two electron irreversible reduction and diffusion controlled process with various sweep rates and pH using different solvent and buffer. From electrochemical data, it was confirmed that the cathodic peak potential affected by sweep rate, media, buffers and pH of the solution. The cyclic voltammograms of zinc complex showed quasi-reversible process for Zn(II)/Zn(I) couple. The antimicrobial activities of synthesized compounds were tested against different bacteria and fungi.

ACKNOWLEDGEMENTS

The authors gratefully thank to the Head, Department of Chemistry, University of Rajasthan for providing the necessary facilities for research.

REFERENCES

1. Das, P.; Linert, W. *Coord. Chem. Rev.*, **2016**, *311*, 1-23.
2. Maher, K. A.; Mohammed, S. R. *Int. J. Cur. Res. Rev.*, **2015**, *7*, 6-16.
3. Antony, R.; David, S. T.; Saravanan, K.; Karuppasamy K.; Balakumar, S. *Spectrochim. Acta A.*, **2013**, *103*, 423-430.
4. Ganjali, M. R.; Pourjavid, M. R.; Rezapour, M.; Poursaberi, T.; Daftari A.; Niasari, M. S. *Electroanal.*, **2004**, *16*, 922-927.
5. Lacroix, P. G. *Eur. J. Inorg. Chem.*, **2001**, *2001*, 339-348.
6. Waddai, F. Y.; Kareem, E. K.; Hussain, S. A. *Orient. J. Chem.*, **2018**, *34*, 434-443.
7. Orojloo, M.; Zolgharnein, P.; Solimannejad, M.; Amani, S. *Inorg. Chim. Acta.*, **2017**, *467*, 227-237.
8. Galini, M.; Salehi, M.; Kubicki, M.; Amiri, A.; Khaleghian, A. *Inorg. Chim. Acta.*, **2017**, *461*, 167-173.
9. Vijayalakshmi, M. *Rasayan J. Chem.*, **2018**, *11*, 857-864.
10. Al-Zaidi, B. H.; Hasson, M. M.; Ismail, A. H. *J. Appl. Pharm. Sci.*, **2019**, *9*, 45-57.
11. Farghaly, O. A.; Hameed, R. S. A.; Abu-Nawwas, A. H. *Int. J. Electrochem. Sci.*, **2014**, *9*, 3287- 3318.
12. Kuate, M.; Conde, M. A.; Mainsah, E. N.; Paboudam, A. G.; Tchieno, F. M. M.; Ketchemen, K. I. Y.; Kenfack, I. T.; Ndifon, P. T. *J. Chem.*, **2020**, *2020*, 1-21.
13. Sherbiny, F. *Az. J. Pharm Sci.*, **2017**, *55*, 88-96.
14. Choudhary, P.; Kumawat, G. L.; Sharma, R.; Varshney, S. *Int. J. Pharm. Sci. Res.*, **2018**, *9*, 4601-4609.
15. Meena, L.; Choudhary, P.; Varshney, A. K.; Varshney, S. *Port. Electrochim. Acta.*, **2019**, *37*, 271-283.
16. Balae, I. C.; Verma N. K.; Jharwal, M.; Meena, S.; Varshney, S. *Orient. J. Chem.*, **2022**, *38*, 318-326.
17. Dhanaraj, C. J.; Johnson, J. *Spectrochim. Acta A Mol. Biomol. Spectrosc.*, **2014**, *118*, 624-631.
18. Kumawat, G. L.; Choudhary, P.; Varshney, A. K.; Varshney, S. *Orient. J. Chem.*, **2019**, *35*, 1117 -1124.
19. Sumrra, S. H.; Ibrahim, M.; Ambreen, S.; Imran, M.; Danish, M.; Rehmani, F. S. *Bioinorg. Chem. Appl.*, **2014**, *2014*, 1-10.
20. Rama, I.; Selvameena, R. *J. Indian Chem. Soc.*, **2020**, *97*, 2144-2154.